Atomically flat aluminum-oxide barrier layers constituting magnetic tunnel junctions observed by in situ scanning tunneling microscopy

doi: 10.1063/1.2108121

Atomically flat aluminum-oxide barrier layers constituting magnetic tunnel junctions observed by *in situ* scanning tunneling microscopy

M. Mizuguchi[a] and Y. Suzuki
Department of Materials Engineering Science, Graduate School of Engineering Science, Osaka University, Toyonaka, Osaka 560-8531, Japan and Core Research for Evolutional Science and Technology (CREST), Japan Science and Technology Agency, Kawaguchi, Saitama 332-0012, Japan

T. Nagahama and S. Yuasa
NanoElectronics Research Institute, National Institute of Advanced Industrial Science and Technology (AIST), Tsukuba, Ibaraki 305-8568, Japan and Core Research for Evolutional Science and Technology (CREST), Japan Science and Technology Agency, Kawaguchi, Saitama 332-0012, Japan

(Received 6 June 2005; accepted 26 August 2005; published online 18 October 2005)

Observation using *in situ* scanning tunneling microscopy of the layers constituting a magnetic tunnel junction with a naturally oxidized aluminum barrier layer revealed an extremely flat aluminum-oxide surface. It was clarified from line-scan images that the aluminum-oxide barrier layer has atomic steps. This flatness, which is surprising given that the aluminum-oxide film is amorphous, reduced electron scattering within the barrier, leading to momentum-dependent tunneling, which should enable the fabrication of advanced devices, such as spin-polarized resonant tunneling transistors. © *2005 American Institute of Physics*. [DOI: 10.1063/1.2108121]

Since the discovery of the tunnel magnetoresistance (TMR) effect,[1] numerous studies on improving the performance of magnetic tunnel junctions (MTJs) have been reported.[2–9] The TMR effect has already been applied to read heads of hard disk drives as a magnetic sensor. Recent advances in growth techniques have led to the discovery of resonant tunneling due to the quantum well effect in MTJs with a single-crystal ferromagnetic bottom electrode.[5,6] The phenomenon is apparently due to the coherent transport of electrons in which the wave vector ($\mathbf{k}_{\parallel}$) is conserved owing to the use of a single-crystal electrode. Moreover, the giant TMR effect even at room temperature (RT) and a significant bias dependence have been obtained in MTJs with crystalline MgO(001) barriers and electrodes.[7–9] While several investigations of the surface structures of barrier layers in MTJs by scanning probe microscopy have been reported,[10–12] the samples had polycrystalline bottom electrodes, and the grains of these electrodes may have created leaks in the aluminum-oxide (Al–O) barriers, which would have degraded the tunneling characteristics. Thus a single-crystalline bottom electrode is indispensable for examining the structures of atomically flat Al–O layers without barrier leaks. Our previous experiments have already revealed that three monolayers of epitaxial aluminum is the minimum thickness to form a tunnel barrier after natural oxidation.

Furthermore, a technique of growing an extremely thin epitaxial ferromagnetic film on insulators is needed for application to various devices such as the gate electrodes of spin-polarized resonant tunneling transistors. Sato and Mizushima reported a spin-valve transistor with an epitaxial Fe/Au/Fe(001) film; however, the efficiency of carrier injection was not very high, and they could not observe the resonant tunneling effect.[13] Therefore, the direct observation of the surface structures of stacked layers that result in optimum growth is crucial for achieving resonant tunneling transistors.

In this letter, we report investigations of the morphologies of the layers constituting MTJs, including an epitaxial bottom electrode layer and an Al–O tunnel barrier layer, by *in situ* scanning tunneling microscopy (STM).

We used MgO(001) single crystals as substrates. Contact electrodes were deposited onto surfaces of substrates to enable the STM observation. The films were grown using a conventional metal molecular-beam epitaxy (MBE) system; Cr, Au, and Fe layers were deposited by electron-beam evaporation of source materials, and Al was deposited using a fusion cell. A vacuum chamber for STM measurements was connected to the MBE chamber under an ultrahigh vacuum, and the samples were transferred between the MBE chamber and STM chamber without being exposed to the air, enabling us to perform *in situ* STM analysis. A tungsten wire was used as a scanning tip, and the surfaces were scanned in constant current mode at RT. The bias voltages applied to the samples were varied between −0.1 and 2 V.

A cross section of the prepared film is schematically illustrated in Fig. 1(a). An Fe(001) layer (a bottom electrode) and an Al(001) layer were grown epitaxially at RT on buffer layers of Au(001)/Cr(001) grown at 573 K. The thickness of each layer was estimated using quartz crystal microbalances within the MBE system. The thickness of the Al layer was set to 0.61 nm, corresponding to three monolayers of Al(001). The Al layer was left in pure oxygen at 100 Torr for 15 min. at RT to form the Al–O barrier layer. We also observed the morphology of an Fe top electrode grown on the barrier layer at RT. The surface of each layer was monitored using reflection high-energy electron diffraction (RHEED) after each STM analysis.

The surface of the Au(001) buffer layer was atomically flat with distinct steps running parallel to the Au[110] direction, as shown in Fig. 1(b). The terrace widths were estimated to be from 10 to 40 nm. The inset shows an atomic resolution image of a terrace part. The reconstructed $(5\times n)$ surface is evident, containing rows of Au atoms with long-period distortion.[14,15] The bottom electrode was grown

[a]Author to whom correspondence should be addressed; electronic mail: mizuguchi@mp.es.osaka-u.ac.jp

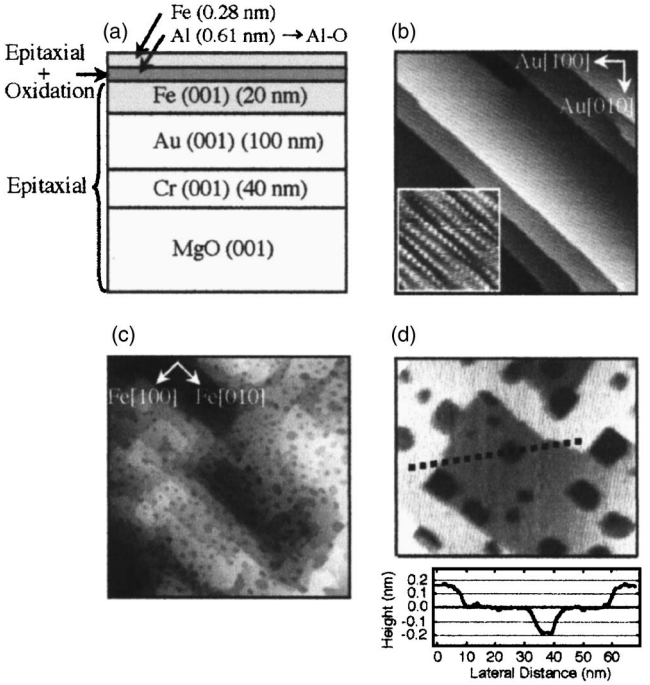

FIG. 1. (a) Sample schematic. Al–O barrier layer was formed by natural oxidation of epitaxially grown Al(001) layer. (b) 100×100 nm STM image of surface of Au(001) layer taken with a bias voltage of −0.1 V and a current of 0.05 nA. Inset shows 5×5 nm zoom in showing atomic resolution at a bias voltage of 0.5 V and a current of 2.0 nA. The STM images of Fe(001) bottom electrode: (c) 500×500 nm and (d) 80×100 nm zoom in with a bias voltage of 1.0 V and a current of 3.0 nA. Line-scan profile corresponds to the dotted line.

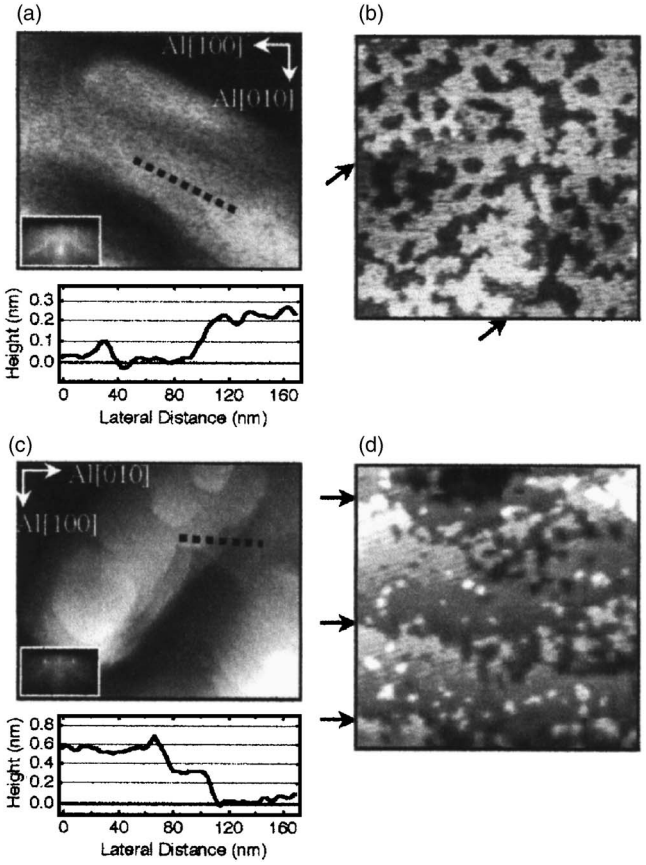

FIG. 2. 400×500 nm STM images of surfaces of (a) Al(001) layer and (c) Al–O layer with a bias voltage of 0.5 V and a current of 0.5 nA. Line-scan profiles correspond to dotted lines. Inset shows the RHEED pattern for each surface. Incident beam was injected in direction parallel to Al[100]. Magnified STM images of (b) Al layer (100×100 nm) with a bias voltage of 0.5 V and a current of 0.5 nA and (d) Al–O layer (40×40 nm) with a bias voltage of 2.0 V and a current of 3.0 nA. The arrows show step edges.

with a thickness of 20 nm on a flat Au(001) layer at RT followed by annealing at 573 K to improve the morphology of the Fe layer [Fig. 1(c)]. It also had a step-and-terrace structure, similar to that of the Au(001) surface. The terrace widths were between 20 and 70 nm, slightly wider than those of the Au surface. Bunching of the Fe steps may have caused this. Several screw dislocation terminating steps were seen. Furthermore, a large number of voids were dispersed over the surface.

Figure 1(d) shows a magnified STM image of the Fe(001) surface with a line-scan profile. The voids are square with depths from 0.15 to 0.18 nm. They may have resulted from the strain between the Au(001) and Fe(001) (lattice mismatch of about 3.7%), although is not very clear at the present stage. The step height was about 0.15 nm. This is very close to the thickness of one Fe(001) monolayer (0.14 nm), meaning that the steps were "atomic steps." To investigate the possible segregation of the Au atoms onto the Fe surface, we performed Auger electron spectroscopy after the annealing of the Fe layer. No significant peaks derived from Au were observed.

We also investigated the surface topology of an Al layer with a thickness of 0.61 nm grown on the Fe(001) layer [Fig. 2(a)]. Rectangular terrace structures of various nanometer sizes were observed, similar to those of the Fe(001) layer. This shape is thought to reflect that of the underlying Fe steps. A streaky RHEED pattern was observed, showing fine epitaxial growth of fcc Al(001). The terrace widths and step height estimated from a line profile were from 80 to 120 nm and 0.2 nm, respectively. This step height corresponds exactly to one monolayer of Al(001), indicating that the Al(001) layer has atomic steps. Figure 2(b) shows an enlarged image of the Al(001) surface; the arrows running in the same directions show the step edges. The epitaxial Al(001) layer formed a *network* structure.

The surface of an oxidized Al(001) layer was considerably different from that of an unoxidized one, as shown in Figs. 2(c) and 2(d). A RHEED pattern captured after oxidation showed a halo with very weak streaks from the buried Fe(001) layer. While the Al–O film is known to be *amorphous* from cross-section transmission electron microscopy,[6] considerably flat surface structures with steps were observed for the Al–O surface. The terrace widths were estimated to be from 20 to 200 nm. The step heights estimated from a line-scan image (0.25–0.3 nm) were greater than that of Al(001) (0.2 nm). Since naturally oxidized aluminum has 1.3–1.5 times the height of pure aluminum, we can conclude that the Al(001) layer was thoroughly oxidized. Moreover, the edges of the terrace steps changed from squarish to roundish due to the oxidation. The formation of a very flat barrier layer by natural oxidation is attractive; moreover, distinct step edges were observed, as indicated by the arrows in the magnified STM image shown in Fig. 2(d), which signifies ideal layer-by-layer growth. The large monoatomic terraces of barrier layers have not been previously reported, even for crystalline MgO barriers grown on Fe whiskers, which have extremely large terraces.[10]

A STM image [Fig. 3(a)] after the growth of two monolayers (MLs) of Fe [0.28 nm for Fe(001)] on the amorphous

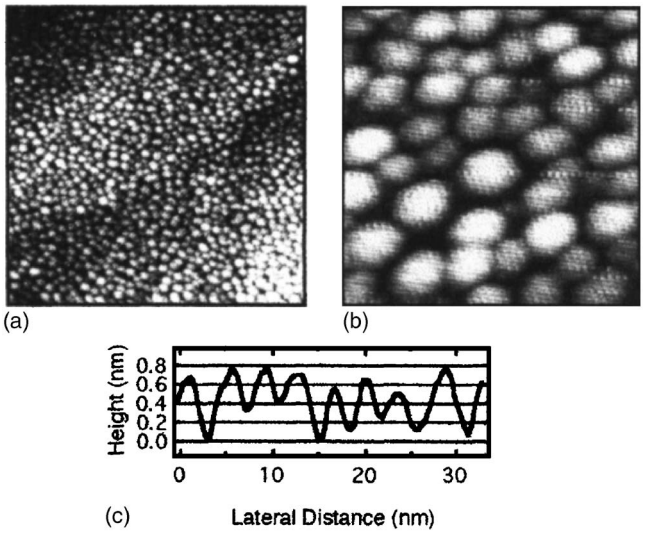

FIG. 3. STM images of Fe(001) top electrode: (a) 100×100 nm with a bias voltage of 2.0 V and a current of 1.5 nA and (b) 20×20 nm zoom in with a bias voltage of 0.5 V and a current of 0.25 nA. (c) Line-scan profile of Fe(001) top electrode.

Al–O layer showed slight steps and terraces and complete island growth. A weak ring RHEED pattern with a few spots was observed after the growth of Fe; it indicates the formation of a polycrystalline film with some prior crystallographic alignments. Figure 3(b) shows a magnified image of the Fe top layer. The Fe clusters were almost round, averaged 3–5 nm in diameter, and had a density of about $1.0\times10^{13}/\mathrm{cm}^2$, indicating they were packed rather closely. A line-scan profile of the Fe top electrode is shown in Fig. 3(c). The Fe clusters had heights between 0.4 and 0.7 nm, meaning that they had three, four, or five MLs, and the heights were more than the nominal thickness.

Direct observation of each layer in the MTJs confirmed that epitaxial growth of the Fe bottom electrode and a very flat barrier are the keys to coherent electron tunneling. The achievement of the extremely flat barrier layer may have been because the natural oxidation advances very mildly, so the epitaxial Al layer remains flat even after oxidation. This slow oxidation could have prompted the migration of atoms, causing the roundish step edges to become clearer than those of the pure Al layer. Moreover, no grains were seen in the Al–O surface, so we can conclude that the oxidation from Al grains did not proceed and that the Al layer was uniformly oxidized. This flatness probably reduced the scattering of electrons within the barrier, resulting in the spin-polarized resonant tunneling phenomenon.

The topology of the top Fe layer was independent of that of the Al–O barrier, judging from the cross sections, so the individual three-dimensional growth of the Fe apparently advanced due to poor wettability. Island growth, very similar to that of two MLs Fe, was also observed for one-ML Fe film, so optimization of the growth conditions, including the substrate temperature and control of wettability, is indispensable to obtaining a flat top electrode on the Al–O barrier layer.

In conclusion, *in situ* STM observation of the various layers constituting a magnetic tunnel junction revealed, for the first time, an amorphous Al–O barrier layer with a step-and-terrace structure. The step height of the barrier was estimated to be 0.3 nm from the STM images. This value corresponds exactly to that of one atomic layer of Al_2O_3 crystal. This extremely flat barrier enabled spin-polarized resonant tunneling transport. The top electrode of Fe showed three-dimensional growth. It is thus necessary to optimize the growth conditions to achieve a fully epitaxial TMR junction with an Al–O barrier.

The authors are grateful to M. Yamamoto of AIST for assisting with the experiments. This work was partly supported by The 21st Century COE Program (G18) of the Japan Society for the Promotion of Science.

[1] T. Miyazaki and N. Tezuka, J. Magn. Magn. Mater. **139**, L231 (1995); J. S. Moodera, L. R. Kinder, T. M. Wong, and R. Meservey, Phys. Rev. Lett. **74**, 3273 (1995).
[2] S. Yuasa, T. Sato, E. Tamura, Y. Suzuki, H. Yamamori, K. Ando, and T. Katayama, Europhys. Lett. **52**, 344 (2000).
[3] K. Inomata, S. Okamura, R. Goto, and N. Tezuka, Jpn. J. Appl. Phys., Part 2 **42**, L419 (2003).
[4] Y. Fukumoto, K. I. Shimura, A. Kamijo, S. Tahara, and H. Yoda, Appl. Phys. Lett. **84**, 233 (2004).
[5] T. Nagahama, S. Yuasa, Y. Suzuki, and E. Tamura, Appl. Phys. Lett. **79**, 4381 (2001).
[6] S. Yuasa, T. Nagahama, and Y. Suzuki, Science **297**, 234 (2002).
[7] S. Yuasa, A. Fukushima, T. Nagahama, K. Ando, and Y. Suzuki, Jpn. J. Appl. Phys., Part 2 **43**, L588 (2004).
[8] S. S. P. Parkin, C. Kaiser, A. Panchula, P. M. Rice, B. Hughes, M. Samant, and S. H. Yang, Nat. Mater. **3**, 862 (2004).
[9] S. Yuasa, T. Nagahama, A. Fukushima, Y. Suzuki, and K. Ando, Nat. Mater. **3**, 868 (2004).
[10] W. Wulfhekel, M. Klaua, D. Ullmann, F. Zavaliche, J. Kirschner, R. Urban, T. Monchesky, and B. Heinrich, Appl. Phys. Lett. **78**, 509 (2001).
[11] M. Hayashi, Y. Ando, and T. Miyazaki, Jpn. J. Appl. Phys., Part 2 **40**, L1317 (2001).
[12] Y. Ando, M. Hayashi, S. Iura, K. Yaoita, C. C. Yu, H. Kubota, and T. Miyazaki, J. Phys. D **35**, 2415 (2002).
[13] R. Sato and K. Mizushima, Appl. Phys. Lett. **79**, 4381 (2001).
[14] X. Gao, A. Hamelin, and M. J. Weaver, Phys. Rev. Lett. **67**, 618 (1991).
[15] J. de la Figuera, M. A. González, R. García-Martínez, J. M. Rojo, O. S. Hernán, A. L. Vázquez de Parga, and R. Miranda, Phys. Rev. B **58**, 1169 (1998).